Tomato-plant Sunlit-leaf Segmentation Using Convolutional Neural Networks: Supporting Crop Water Stress Index Measurements

Jacob Hampton,[1] Athanasios Aris Panagopoulos,[1] Minas Pantelidakis,[2] Eric Kor,[1] Konstantinos Mykoniatis,[2] Orestis P. Panagopoulos,[3] Shawn Ashkan[4]

[1] Department of Computer Science, California State University Fresno
[2] Department Industrial and Systems Engineering, Auburn University
[3] Department of Management Information Systems, California State University Stanislaus
[4] Center for Irrigation Technology, California State University Fresno
jacobhampton@mail.fresnostate.edu, apanagopoulos@mail.fresnostate.edu, mzp0122@auburn.edu, mzk0141@auburn.edu
opanagopoulos@csustan.edu, koreric@mail.fresnostate.edu, sashkan@mail.fresnostate.edu

Abstract

Many precision irrigation approaches rely on calculating the crop water stress index (CWSI) using measurements of the sunlit-leaf canopy temperature (*sunlit-leaf* T_c). To this end, they typically employ machine learning and/or statistical techniques along with visible-spectrum and/or thermal imagery to identify the *sunlit-leaf* region and its temperature. The precise segmentation of sunlit leaves is of utmost importance; considering non-sunlit leaves while calculating CWSI, can lead to inaccurate and inefficient under-irrigation or over-irrigation. Recent work demonstrated that convolutional neural networks (CNN) can support highly precise sunlit leaf segmentation in pistachio trees. The same work introduced a complete methodology for the estimation of CWSI in pistachio trees and released a corresponding free-of-charge web tool: CIWA. However, the generality of the approach to other crops is not discussed. Here, we extend the CIWA methodology to tomato plants. We discuss the challenges of extending the CIWA approach to shorter plants and release the first annotated dataset for sunlit-leaf segmentation in tomato plants. We consider three CNN architectures for this task: FRRN-A, FC-DenseNet103 and ResNet101-DeepLabV3, and show that FC-DenseNet103 is the most suitable for the task. Based on these results, we introduce an extended CIWA release to enable tomato CWSI measurements.

Introduction

The world population is set to increase by more than $\sim$25% during the next three decades. The demand for agricultural products is expected to increase significantly alongside to meet the growing needs (Food and Agriculture Organization 2012; Fess, Kotcon, and Benedito 2011). The vast majority of harvested agricultural production is depended on water found in groundwater and surface water sources (Ozdogan et al. 2010). Freshwater is a small fraction of all water, and the latest harsh climate changes, make it a scarce resource for many countries (Konikow 2013; Nations 2014; Rockström et al. 2017). Therefore, managing freshwater supplies has become increasingly important in recent years. Precision irrigation has been heralded as a key means towards a sustainable future as it aims to obtain optimal usage of water resources (Abioye et al. 2020).

Many precision irrigation approaches rely on calculating the crop water stress index (CWSI). CWSI measures the relative transpiration rate occurring from a crop based on environmental parameters as well as the canopy temperature, T_c (Jackson et al. 1981). Due to this reason a T_c measurement is a critical component of such methods. Importantly though, T_c is considerably affected by whether sunlit or non-sunlit leaves are primarily considered. Incorporating T_c measurements based only on sunlit leaves is crucial for irrigation-related applications (Alchanatis et al. 2011; Gardner, Nielsen, and Shock 1992). This is the case as sunlit leaves get under-water stressed sooner and to a greater extent compared to non-sunlit ones (Alchanatis et al. 2011; Gardner, Nielsen, and Shock 1992). T_c measurements based on non-sunlit leaves can considerably under-or-over-estimate the CWSI. Precise sunlit-leaf segmentation is a critical challenge for *sunlit-leaf* T_c measurements for precision irrigation. Notably, precise *sunlit-leaf* T_c measurements can also support applications in various domains outside precision irrigation ranging from plant-disease monitoring to microclimate and physiological process modeling (e.g., Cui et al. 2010; Dai, Dickinson, and Wang 2004; Wang et al. 2017).

Recently, the work of Pantelidakis et al. 2022 utilized visible spectrum and thermal imagery to successfully measure the *sunlit-leaf* T_c of pistachio trees. The work proposed a two-step methodology where the sunlit leaves are segmented in visible spectrum images and the respective region on corresponding thermal images is used to calculate *sunlit-leaf* T_c. Pantelidakis et al. 2022 showed that convolutional neural networks (CNNs) can be successfully used to identify sunlit-leaf regions in pistachio tree visible-spectrum images with high precision and accuracy. That work also introduced a web-based tool to support CWSI calculations of pistachio trees, namely CIWA. Nevertheless, how well the approach and methodology extends to other crops is not discussed.

In this work, we extend the CIWA approach considering tomato plants. We release the first annotated dataset for sunlit-leaf segmentation in tomato plants and make it publicly available to the research community (www.apanagopoulos.com/ciwa). We provide a thorough evalua-

tion of three CNN architectures, namely FRRN-A (Pohlen et al. 2017), FC-DenseNet103 (Jégou et al. 2017) and ResNet101-DeepLabV3 (Chen et al. 2017b), for this task. We show that FC-DenseNet103 is the most suitable architecture and that it can achieve high accuracy and precision (of 0.853 and 0.703, respectively). We also discuss the challenges of the methodology when moving from tall trees, such as pistachios, to shorter ones, such as tomatoes. Finally, in the context of this work we extend the online tool released by Pantelidakis et al. 2022 to provide free-of-charge measurements of the CWSI of tomato plants.

The rest of the paper is structured as follows. First, we discuss background material. Then, we discuss the challenges when extending CIWA beyond tall trees. We continue by introducing our dataset and, subsequently, we discuss our approach and our CNN selection methodology. Then, we discuss the results and the extension of the CIWA web-based tool. Finally we conclude and discuss future work directions.

The CIWA Methodology

Accurate *sunlit-leaf* T_c measurements can support numerous applications including CWSI measurements for precision irrigation (as well as plant-disease monitoring and microclimate and physiological process modeling (Dai, Dickinson, and Wang 2004; Cui et al. 2010; Wang et al. 2017)). Segmenting sunlit leaves is a prominent challenge. Manually segmenting sunlit-leaves is a process that is labor intensive, time consuming and prone to mistakes. Works that segment sunlit leaves using statistical and machine learning techniques are emerging, over the past years.

The work of Pantelidakis et al. 2022 proposed a complete methodology for estimating the CWSI of pistachio plants based on three steps. First, the sunlit leaves of pistachio trees are segmented in visible spectrum images using CNNs. Then the derived mask is utilized to extract the corresponding region from corresponding infrared-spectrum images and calculate the *sunlit-leaf* T_c as the average temperature. Finally this measurement along with environmental variables are used to calculate the CWSI of pistachio plants. That work also released a free-of-charge web-based tool that implements the aforementioned methodology (https://www.apanagopoulos.com/ciwa). Nevertheless, how well this approach extends to other crops is not detailed or documented.

CNNs for Semantic Segmentation

Semantic segmentation considers the task of identifying what is present in an image and where by finding all pixels that belong to it. Deep neural networks which consist of multiple layers are among the most advanced machine learning techniques for semantic segmentation (Han et al. 2020; Wang et al. 2016; Deng et al. 2017; Alzubaidi et al. 2021)

The training of CNNs tends to be a tedious process that demands many resources. To alleviate that, transfer learning may be used. Transfer learning is achieved by using a set of pre-trained layers that are fixed during training and are sometimes referred to as the back-bone (Majurski et al. 2019; Atkinson et al. 2020). The back-bone is trained on a large dataset, such as ImageNet (Deng et al. 2009) and extracts features for image analysis. The remaining model is then trained on a more specific, smaller, dataset such as the sunlit-leaf segmentation dataset we use on this paper (Weiss, Khoshgoftaar, and Wang 2016). By doing so, transfer learning can effectively reduce the training time (Weiss, Khoshgoftaar, and Wang 2016; Kanavati and Tsuneki 2021).

Many CNN design techniques have been proposed for the task of semantic segmentation over the past years (Briot, Viswanath, and Yogamani 2018). FRRN-A, or Full-Resolution Residual Network was proposed by (Pohlen et al. 2017). It utilizes two computation streams which are combined using Full-Resolution Residual Units to achieve good localization and recognition performance. Without pre-training or additional processing, FRRN-A has been shown to achieve good semantic segmentation performance on a number of demanding datasets, including the PTSL20 dataset (Pantelidakis et al. 2022), which considers sunlit-leaf segmentation for pistachio trees. Due to these reasons this architecture is considered in this work.

FC-DenseNet103 (Jégou et al. 2017) extends DenseNet (Huang et al. 2017) by including an upsampling path to support semantic segmentation. The architecture has shown to achieve very good segmentation performance without pre-training on a number of demanding datasets including PTSL20 (Pantelidakis et al. 2022). For these reasons this architecture is also considered in this work.

ResNet101-DeepLabV3 (Chen et al. 2017b) uses atrous convolution (Papandreou, Kokkinos, and Savalle 2015; Sermanet et al. 2013) to extract dense features for semantic segmentation. DeepLabV3 typically utilizes a pretrained backbone, in our case ResNet101 (shown to perform better than the less deep ResNet-50 (Chen et al. 2017a)), which is trained on the ImageNet dataset (Deng et al. 2009). The architecture has shown to achieve very good segmentation performance on a number of demanding datasets including PTSL20 (Pantelidakis et al. 2022). For these reasons we employ this architecture in this work.

Extending CIWA to Short Plants: the Challenges

In this work we extend the CIWA methodology of Pantelidakis et al. 2022 for tomato plants. We note here that despite the many similarities, identifying sunlit leaves in pistachio trees has also some key differences when compared to the same task for shorter plants such as tomato plants. The main difference among them is that pictures of tomato plants are typically taken from above. Hence, sunlit leaves consider a great proportion of the image. On the other hand, pictures of tall trees, including the pistachio trees in the original CIWA work, are taken from below and, as such, sunlit leaves consider only a small portion of the image. Nevertheless, when picture taken from below, sunlit leaves are typically captured with the sky as the background with typically well defined boundaries. This makes it somewhat easier to distinguish compared to the same task when pictures are taken from above. When a picture is taken from above, sunlit leaves are seen mainly with the ground and other leaves as the background. Distinguishing sunlit-leaves can be much

more challenging in this case due to the similar color distributions. Hence, the performance of the CNN architectures considered can differ. Furthermore, the high temperature of the ground, compared to the low one of the sky, can lead to a significant overestimation of the canopy temperature in case of miss-classification. This renders precise segmentation an even more prominent requirement.

A New Dataset for Tomato-plant Sunlit-leaf Segmentation

A distinct contribution of this work is the release of the first annotated dataset for sunlit-leaf semantic segmentation in tomato plants: TMSL21. The TMSL21 dataset is made publicly available to the community at www.apanagopoulos/ciwa. TMSL21 considers tomato plants and includes visible-spectrum images and corresponding sunlit leaf labels. The dataset comes complete with a corresponding infrared spectrum image that includes calibrated FLIR AX8 thermal camera metadata to further support precision irrigation and related research. In more detail, the dataset considers 808 data entries. Each data entry includes the following:

- A 504X286 visible-spectrum image. A sample image is illustrated in Figure 2a
- A 504X286 corresponding label for segmenting tomato sunlit leaves. The pixels in this mask fall in one of two categories: sunlit leaves or non-sunlit leaves. A sample image is illustrated in Figure 2b
- A 80X60 FLIR AX8 file image that includes an embedded visible-spectrum image, an embedded infrared image, and FLIR AX8 metadata. We note that the metadata provided are PTSL20-specific and calibrated. In particular, atmospheric temperature and humidity data are collected via local weather stations. The emissivity of the crop and the reflected temperature of surrounding objects is empirically estimated while the distance from the object is manually calculated. The remaining metadata retain their default values. For a full list of the metadata please refer to FLIR AX8 documentation (Flir 2022).

The dataset was collected over the summer of 2021 in the region of San Joaquin Valley, California, USA using a FLIR AX8 thermal camera and local weather stations. All pictures are taken from the ground level, which makes our methodology applicable without the need of drones or other means to acquire aerial images. TMSL21 is annotated manually by experts and trained personnel. Notably, unsupervised clustering has been used as a way to support the labor intensive manual annotation process as in Pantelidakis et al. 2022

Selecting a CNN Model

We consider and evaluate three CNN architectures on the TMSL21 dataset, namely FRRN-A (Pohlen et al. 2017), FC-DenseNet103 (Jégou et al. 2017) and ResNet101-DeepLabV3 (Chen et al. 2017b). We do this to identify the most suitable model for incorporation into the CIWA online tool. We selected these CNN architectures as those have achieved good performance in pistachio trees (Pantelidakis et al. 2022). All architectures are considered with the same design characteristics as in Pantelidakis et al. 2022

The TMSL21 dataset was randomly split into training (557 images), validation (183 images), and test (68 images) set. The validation set was used to execute early stopping and avoid over-fitting (Prechelt 1998). All approaches have been trained using a softmax cross entropy loss function between per-label activations (logits) and labels. All architectures have been trained using RMSProp with a learning and decay rate of 0.0001 and 0.995 respectively.

For all approaches, the performance is measured in terms of accuracy (AC), precision (PR), recall (RC), F1 score, and mean intersection-over-union ($\overline{\text{IoU}}$). Precision is arguably the most important metric when it comes to sunlit-leaf segmentation for precision irrigation. The inclusion of non-sunlit leaves can significantly underestimate T_c and CWSI. Sunlit leaves are the ones that demonstrate stress more timely and to a greater extent, ultimately meaning that underestimation can lead to inefficient irrigation.

Results and Discussion

All evaluation metrics results are reported in Table 1. Figure 1 illustrates the confusion matrices while Figure 2 illustrates example segmentations, for all approaches. All models demonstrate good performance. FC-DenseNet103 and FRRN-A seem to perform better than ResNet101-DeepLabV3. This is evident by the results in all metrics considered and, especially, the recall metric which leads to a poor F1 score for ResNet101-DeepLabV3. As illustrated in Figure 1c, ResNet101-DeepLabV3 has the lowest number of sunlit leaves that are accurately classified as sunlit ones, compared to the rest methods. However, although $\sim$12.89% of all pixels are miss-classified as non-sunlit-leaf ones, only $\sim$4.85% are miss-classified as sunlit-leaf ones. As such, even though the ResNet101-DeepLabV3 precision is lower than the other CNN models, the gap is not that great. Nevertheless, ResNet101-DeepLabV3 is a poorer choice overall. As can be seen in Figure 2e, ResNet101-DeepLabV3 demonstrates worse fine-grain boundary adherence compared to the rest of the models.

When comparing FRRN-A to FC-DenseNet103, the latter seems to achieve better performance in all metrics except for precision. As discussed, precision is the most important metric for this task. However, the difference in precision between FRRN-A and FC-DenseNet103 is minimal and FC-DenseNet103 is superior to FRRN-A in all other metrics. Therefore, we select FC-DenseNet103 for our inclusion in our methodology. As can be seen in Figures 2c and 2d, both FRRN-A and FC-DenseNet103 demonstrate good fine-grain boundary adherence and segmentation performance.

These results are in some alignment with the work of Pan-

	AC	PR	RC	F1	$\overline{\text{IoU}}$
FRRN-A	0.844	**0.706**	0.450	0.550	0.604
FC-DenseNet103	**0.853**	0.703	**0.492**	**0.578**	**0.622**
ResNet101--DeepLabV3	0.823	0.613	0.373	0.464	0.555

Table 1: Performance metrics.

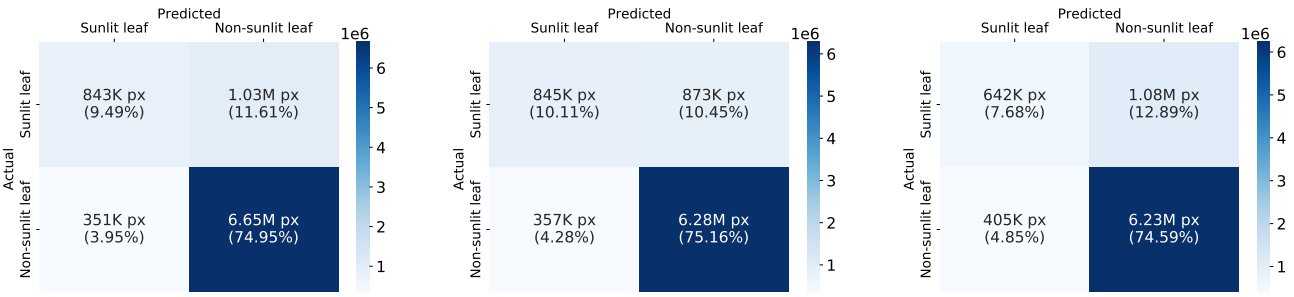

(a) FRRN-A (b) FC-DenseNet103 (c) ResNet101-DeepLabV3

Figure 1: Confusion matrices with the number and percentages of pixels that are appropriately classified per class

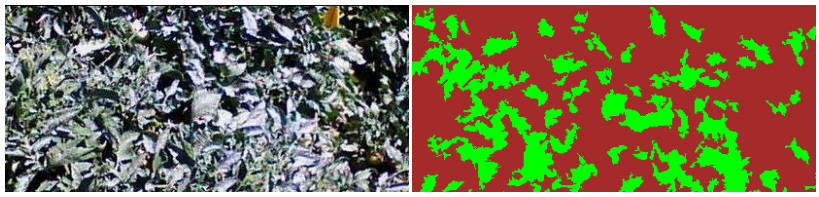

(a) Visible-spectrum image (b) Label (ground truth)

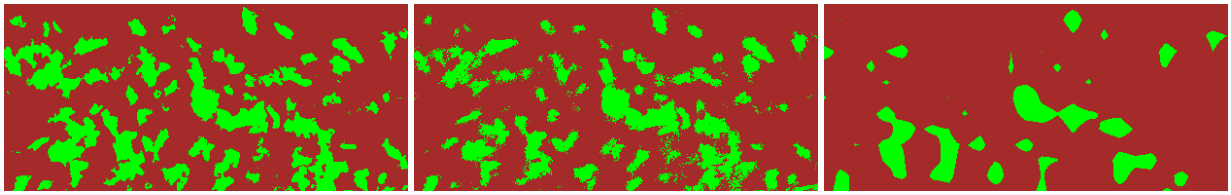

(c) FRRN-A (d) FC-DenseNet103 (e) ResNet101-DeepLabV3

Figure 2: Sample visible spectrum image and label (ground truth) along with corresponding predictions

telidakis et al. 2022 in pistachio trees. Pantelidakis et al. 2022 demonstrated the effectiveness of all architectures considered here, however it showed FRRN-A to be the winner. We believe that these differences are quite small to be of outmost significance but could demonstrate the variability in the performance of various architectures in slightly but significantly (non-trivially) different tasks. FC-DenseNet103 allows for more fine-grain boundary adherence compared to FRRN-A. This seems to be providing an advantage when pictures are taken from above and the adjacent regions seem to be more similar. Nevertheless the same property could be becoming a disadvantage when the sunlit leaves have clearer boundaries to the background due to the color distribution.

Extending CIWA

The trained FC-DenseNet103 model was used to extend the CIWA web-based tool (Pantelidakis et al. 2022) to tomato plants. In addition, a CWSI calculation for tomato plants was used (Idso et al. 1981). We defer the details to an extended version of this paper. The extended tool can be accessed online, free-of-charge at www.apanagopoulos.com/ciwa. We envisage the tool to be used by the scientific community for related research and by the wider public to support sustainable agriculture practices.

Conclusion

In this work we extended the CIWA methodology for tomato plants. We released the first annotated dataset for sunlit-leaf segmentation in visible-spectrum images of tomato plants. We also evaluated the most promising CNN architectures considered in CIWA (i.e., FRRN-A, FC-DenseNet103, and ResNet101-DeepLabV3) to show that FC-DenseNet103 is a slightly better choice for the task of sunlit-leaf segmentation in tomato plants. We also released an extension of the online CIWA tool for measuring the CWSI of tomato plants. Possible future work directions include experimenting with more CNN architectures for the task of sunlit-leaf segmentation as well as with additional crops.

Acknowledgement

This research was partially funded by the Agriculture Research Institute. The authors would like to thank Enrique Verduzco III, Jacob Whitlow and Aafreen Chhipa for their help in the labeling process.

References

Abioye, E. A.; Abidin, M. S. Z.; Mahmud, M. S. A.; Buyamin, S.; Ishak, M. H. I.; Abd Rahman, M. K. I.; Otuoze, A. O.; Onotu, P.; and Ramli, M. S. A. 2020. A review on monitoring and advanced control strategies for precision irrigation. *Computers and Electronics in Agriculture*, 173: 105441.

Alchanatis, V.; Cohen, A.; Cohen, Y.; Levi, O.; and Naor, A. 2011. Multimodal remote sensing for enhancing detection of spatial variability in agricultural fields. In *Spatial2 Conference: Spatial Data Methods for Environmental and Ecological Processes, Foggia (IT), 1-2 September 2011*, 1–4. Università degli studi di Bergamo.

Alzubaidi, L.; Zhang, J.; Humaidi, A. J.; Al-Dujaili, A.; Duan, Y.; Al-Shamma, O.; Santamaría, J.; Fadhel, M. A.; Al-Amidie, M.; and Farhan, L. 2021. Review of deep learning: Concepts, CNN architectures, challenges, applications, future directions. *Journal of big Data*, 8(1): 1–74.

Atkinson, G. A.; Zhang, W.; Hansen, M. F.; Holloway, M. L.; and Napier, A. A. 2020. Image segmentation of underfloor scenes using a mask regions convolutional neural network with two-stage transfer learning. *Automation in Construction*, 113: 103118.

Briot, A.; Viswanath, P.; and Yogamani, S. 2018. Analysis of efficient cnn design techniques for semantic segmentation. In *Proceedings of the IEEE Conference on Computer Vision and Pattern Recognition Workshops*, 663–672.

Chen, L.-C.; Papandreou, G.; Kokkinos, I.; Murphy, K.; and Yuille, A. L. 2017a. Deeplab: Semantic image segmentation with deep convolutional nets, atrous convolution, and fully connected crfs. *IEEE transactions on pattern analysis and machine intelligence*, 40(4): 834–848.

Chen, L.-C.; Papandreou, G.; Schroff, F.; and Adam, H. 2017b. Rethinking Atrous Convolution for Semantic Image Segmentation. arXiv:1706.05587.

Cui, D.; Zhang, Q.; Li, M.; Hartman, G. L.; and Zhao, Y. 2010. Image processing methods for quantitatively detecting soybean rust from multispectral images. *Biosystems engineering*, 107(3): 186–193.

Dai, Y.; Dickinson, R. E.; and Wang, Y.-P. 2004. A two-big-leaf model for canopy temperature, photosynthesis, and stomatal conductance. *Journal of climate*, 17(12): 2281–2299.

Deng, J.; Dong, W.; Socher, R.; Li, L.-J.; Li, K.; and Fei-Fei, L. 2009. Imagenet: A large-scale hierarchical image database. In *2009 IEEE conference on computer vision and pattern recognition*, 248–255. Ieee.

Deng, L.; Yang, M.; Qian, Y.; Wang, C.; and Wang, B. 2017. CNN based semantic segmentation for urban traffic scenes using fisheye camera. In *2017 IEEE Intelligent Vehicles Symposium (IV)*, 231–236. IEEE.

Fess, T. L.; Kotcon, J. B.; and Benedito, V. A. 2011. Crop breeding for low input agriculture: a sustainable response to feed a growing world population. *Sustainability*, 3(10): 1742–1772.

Flir. 2022. Flir AX8 datasheet.

Food; and Agriculture Organization, U. N. 2012. World Agriculture Towards 2030/2050: The 2012 revision.

Gardner, B.; Nielsen, D.; and Shock, C. 1992. Infrared thermometry and the crop water stress index. II. Sampling procedures and interpretation. *Journal of production agriculture*, 5(4): 466–475.

Han, K.; Wang, Y.; Chen, H.; Chen, X.; Guo, J.; Liu, Z.; Tang, Y.; Xiao, A.; Xu, C.; Xu, Y.; et al. 2020. A survey on visual transformer. *arXiv e-prints*, arXiv–2012.

Huang, G.; Liu, Z.; Van Der Maaten, L.; and Weinberger, K. Q. 2017. Densely connected convolutional networks. In *Proceedings of the IEEE conference on computer vision and pattern recognition*, 4700–4708.

Idso, S. B.; Jackson, R. D.; Pinter, P. J.; Reginato, R. J.; and Hatfield, J. L. 1981. Normalizing the Stress-Degree-Day Parameter for Environmental Variability. *Agricultural Meteorology*, 24: 45–55.

Jackson, R. D.; Idso, S. B.; Reginato, R. J.; and Pinter, P. J. 1981. Canopy Temperature as a Crop Water Stress Indicator. *Water Resources Research*, 17(4): 1133–1138.

Jégou, S.; Drozdzal, M.; Vazquez, D.; Romero, A.; and Bengio, Y. 2017. The one hundred layers tiramisu: Fully convolutional densenets for semantic segmentation. In *Proceedings of the IEEE conference on computer vision and pattern recognition workshops*, 11–19.

Kanavati, F.; and Tsuneki, M. 2021. Partial transfusion: on the expressive influence of trainable batch norm parameters for transfer learning. In *Medical Imaging with Deep Learning*, 338–353. PMLR.

Konikow, L. 2013. Groundwater depletion in the United States (1900 to 2008).

Majurski, M.; Manescu, P.; Padi, S.; Schaub, N.; Hotaling, N.; Simon Jr, C.; and Bajcsy, P. 2019. Cell image segmentation using generative adversarial networks, transfer learning, and augmentations. In *Proceedings of the IEEE/CVF Conference on Computer Vision and Pattern Recognition Workshops*, 0–0.

Nations, U. 2014. WWDR2014.

Ozdogan, M.; Yang, Y.; Allez, G.; and Cervantes, C. 2010. Remote sensing of irrigated agriculture: Opportunities and challenges. *Remote sensing*, 2(9): 2274–2304.

Pantelidakis, M.; Panagopoulos, A. A.; Mykoniatis, K.; Ashkan, S.; Eravi, R. C.; Pamula, V.; Verduzco III, E. C.; Babich, O.; Panagopoulos, O. P.; and Chalkiadakis, G. 2022. Identifying sunlit leaves using Convolutional Neural Networks: An expert system for measuring the crop water stress index of pistachio trees. *Expert Systems with Applications*, 209: 118326.

Papandreou, G.; Kokkinos, I.; and Savalle, P.-A. 2015. Modeling local and global deformations in deep learning: Epitomic convolution, multiple instance learning, and sliding window detection. *CVPR*.

Pohlen, T.; Hermans, A.; Mathias, M.; and Leibe, B. 2017. Full-Resolution Residual Networks for Semantic Segmentation in Street Scenes. In *Computer Vision and Pattern Recognition (CVPR), 2017 IEEE Conference on*.

Prechelt, L. 1998. Early stopping-but when? In *Neural Networks: Tricks of the trade*, 55–69. Springer.

Rockström, J.; Williams, J.; Daily, G.; Noble, A.; Matthews, N.; Gordon, L.; Wetterstrand, H.; DeClerck, F.; Shah, M.; Steduto, P.; de Fraiture, C.; Hatibu, N.; Unver, O.; Bird, J.; Sibanda, L.; and Smith, J. 2017. Sustainable intensification of agriculture for human prosperity and global sustainability. *Ambio*, 46(1): 4–17.

Sermanet, P.; Eigen, D.; Zhang, X.; Mathieu, M.; Fergus, R.; and LeCun, Y. 2013. Overfeat: Integrated recognition, localization and detection using convolutional networks. *arXiv preprint arXiv:1312.6229*.

Wang, J.; Yang, Y.; Mao, J.; Huang, Z.; Huang, C.; and Xu, W. 2016. Cnn-rnn: A unified framework for multi-label image classification. In *Proceedings of the IEEE conference on computer vision and pattern recognition*, 2285–2294.

Wang, Z.; Liu, L.; Wang, B.; and Wang, X. 2017. Aerosol Increases both Sunlit and Shaded Leaf Photosynthesis Rate but with Different Mechanisms. In *AGU Fall Meeting Abstracts*, volume 2017, B51F–1879.

Weiss, K.; Khoshgoftaar, T. M.; and Wang, D. 2016. A survey of transfer learning. *Journal of Big data*, 3(1): 1–40.